QCD branch in SANC

A. Andonov[1], A. Arbuzov[2,3], S. Bondarenko[2,3],
P. Christova[3], V. Kolesnikov[3], R. Sadykov[3]

[1] *Bishop Konstantin Preslavsky University, Shoumen, Bulgaria*
[2] *Bogoliubov Laboratory of Theoretical Physics, JINR*
[3] *Dzhelepov Laboratory for Nuclear Problems, JINR*
ul. Joliot-Curie 6, RU-141980 Dubna, Russia

Abstract

The QCD sector of the system SANC is presented. QCD theoretical predictions for several processes of high energy interactions of fundamental particles at the one-loop precision level for up to some 3- and 4-particle processes are implemented.

1 Introduction

The computer system SANC is aimed to carry out semi–automatic calculations at the one-loop precision level of realistic and pseudo–observables for various processes of elementary particle interactions to be investigated at the present and future colliders – Tevatron, LHC, ILC and others.

We created the QCD environment of SANC and started to implement systematically NLO QCD processes filling the **QCD** branch of SANC tree in the same spirit as in Ref. [1].

We created a set of FORM [2] procedures for the analytic calculation of building blocks of QCD such as self-energies of quarks and gluons, vertices with virtual gluons and corresponding counter terms. These blocks are placed into the **QCD** Precomputation level of the system. The FORM programs are accessible via the same menu sequences as for **QED** or **EW** Precomputation.

We consider here the results of implementation of the first processes of the **QCD** branch available in SANC. They are subdivided into **3legs** and **4legs** branches as one can see in Fig. 1. The **3legs** branch contains **b2q** decays, namely: $t \to W\,b$, $W \to u\,\bar{d}$, $W \to c\,\bar{s}$, $Z \to q\,\bar{q}$ and $H \to q\,\bar{q}$. Here **b** and **q** denote any weak `boson` and any `quark`, respectively, b denotes the b-quark.

The **4legs** branch contains **4f** processes. For the latter there is a branch for **Neutral Current** (NC) processes that contains the Drell–Yan process $q\,\bar{q} \to \ell^-\,\ell^+$, and a branch for

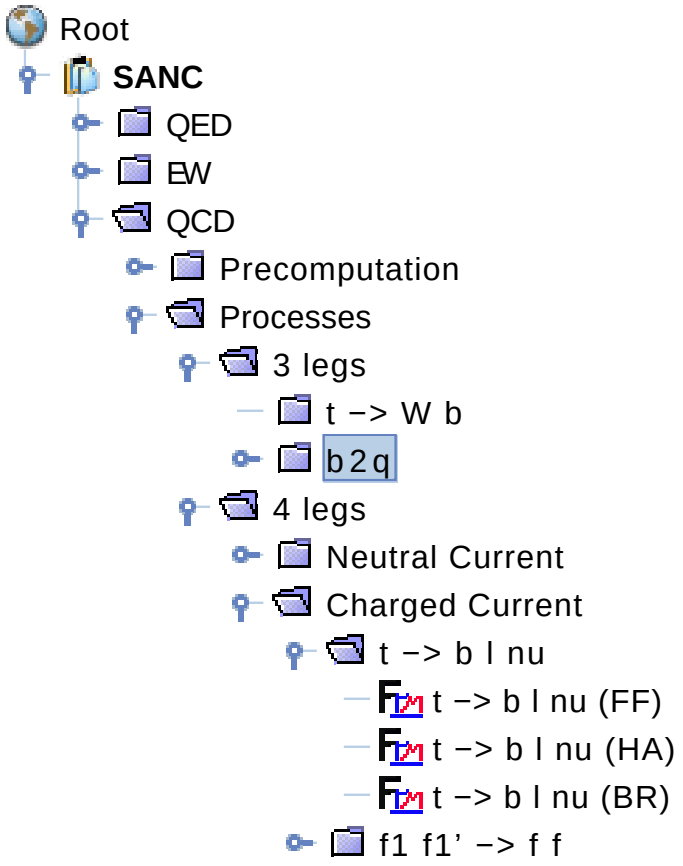

Figure 1: QCD part of the SANC tree.

Charged Current (CC) processes that contains the decay $t \to b\,\ell^+\,\nu_\ell$ and the Drell–Yan $2f \to 2f$ process $u\,\bar{d} \to \ell^+\,\nu_\ell$.

The structure of these branches is the same as the corresponding structure in the **EW** sector of `SANC`. For each process there are three FORM modules: (**FF**) *Form Factor*, (**HA**) *Helicity Amplitudes*, and (**BR**) *Bremsstrahlung*. Using the helicity amplitudes, the `SANC` system calculates numerically the QCD virtual corrections according to the following formula:

$$d\Gamma(d\sigma) \sim \sum_{\lambda_i\lambda_j\lambda_k\lambda_l} \left| \mathcal{H}\left(\mathcal{F}^{\mathbf{Born+1loop}}\right)_{\lambda_i\lambda_j\lambda_k\lambda_l} \right|^2 . \tag{1}$$

Once the three FORM codes for the calculation of (**FF**), (**HA**) and (**BR**) have been compiled and outputs transferred to the software package **s2n.f**, one can get the numerical results. The user guide for running `SANC` is given in Ref. [1].

We convolute the partonic sub-process cross section with quark density functions to get the cross section at the hadronic level. One must avoid double counting of the quark mass singularities, subtracting them from the density functions.

`SANC` version `v1.00` is accessible from servers at Dubna *http://sanc.jinr.ru/ (159.93.74.10)* and CERN *http://pcphsanc.cern.ch/ (137.138.180.42)*.

2 QCD environment

The QCD environment of SANC is a set of FORM procedures relevant for QCD. The basic procedure is `QCDAlgebra.prc`, which calculates color weights for process diagrams. It uses some common relations for T^a matrices and structure constants f^{abc}. We have changed several intrinsic SANC procedures like `FeynmanRules.prc`, `MakeAmpSquare.prc`, `Trace.prc` by including gluon-quark and gluon-gluon vertices in the `FeynmanRules.prc` and giving color indices for quark bispinors. Quarks and leptons bispinors have different representations in SANC.

For example, the Born amplitude of the Drell–Yan process with a charged current taken from procedure `VirtCC4fQCD.prc` is of the following form:

$$\begin{aligned} \mathrm{BornDYCC} &= \frac{1}{8}\, i\, \frac{g^2}{s-\widetilde{M}_W^2} \\ &\times \mathrm{Vb(ii,p1,h1,cl1)}\ \gamma\mathrm{(ii,mu)}\ \gamma 6\mathrm{(ii)}\ \mathrm{U(ii,p2,h2,cl2)}\ \delta\mathrm{(cl1,cl2)} \\ &\times \mathrm{Ub(jj,p3,h3)}\ \gamma\mathrm{(jj,mu)}\ \gamma 6\mathrm{(jj)}\ \mathrm{V(jj,p4,h4)}. \end{aligned} \tag{2}$$

Here U(ii, p2, h2, cl2) and Vb(ii, p1, h1, cl1) are bispinors of the incoming up quark and down antiquark, cl1 and cl2 are their color indices. While Ub(jj, p3, h3) and V(jj, p4, h4) are bispinors of the outgoing lepton pair; γ(ii, mu) and $\gamma 6(\mathrm{ii}) = \mathrm{I(ii)} + \gamma 5(\mathrm{ii})$ are Dirac matrices. Here

$$\widetilde{M}_W^2 = M_W^2 - iM_W\Gamma_W, \tag{3}$$

where M_W is the mass and Γ_W is the width of the W boson.

Using this environment we build a set of precomputation files. The user can find it in the system. To compute the quark self-energy, one follows the sequence:

QCD → Precomputation → Self → Quark → Quark Self

in the QCD tree of `SANC`. Precomputed quark self-energies are used by FORM programs which calculate quark counter terms:

QCD → Precomputation → Self → Quark → QuarkRenConst.

After we have the one-loop amplitude of a given QCD process free from ultraviolet divergences, we can obtain a virtual radiative correction using the universal procedure `MakeAmpSquare.prc` to calculate the modulus squared of the amplitude.

3 QCD radiative correction to b2q decays

We started to work with simple processes of boson decays suitable to test the QCD environment of `SANC`. One-loop Feynman diagrams (see Fig. 2) of these processes contain only a vertex with one virtual gluon and two quark legs, and corresponding QCD counter terms.

Following the standard procedure of SANC, we calculate the virtual part of QCD corrections to these boson decays.

The real part of QCD corrections is created by gluon emission from every quark leg (see Fig. 3).

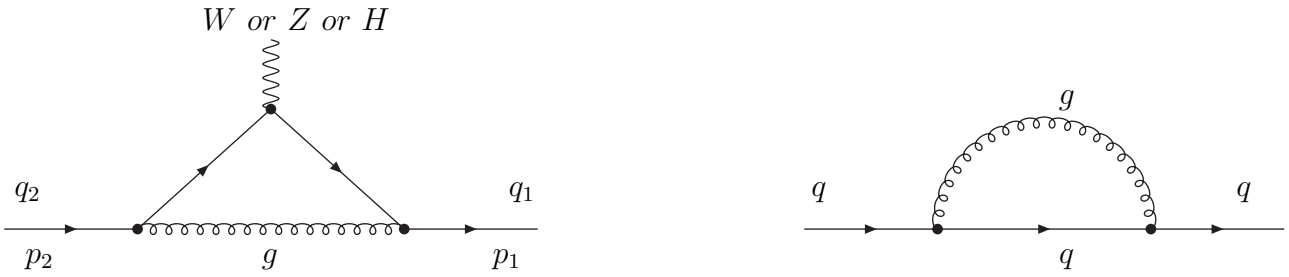

Figure 2: QCD vertex with two quark legs and self energy for quarks.

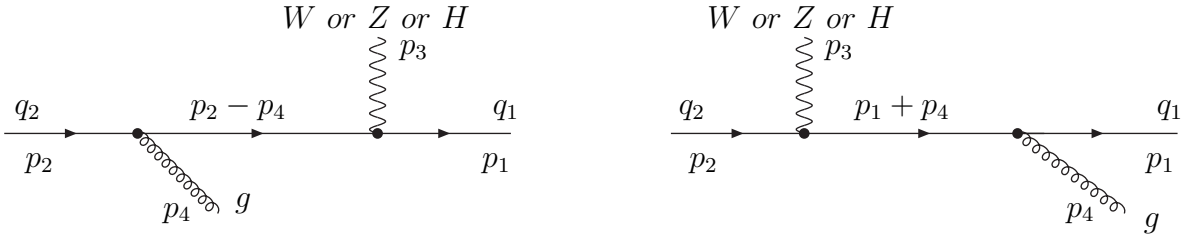

Figure 3: Gluon bremsstrahlung from two quark legs.

Gluon bremsstrahlung implementation needs another set of procedures, specific for every process. Procedures `BremWqqQCD.prc`, `BremZqqQCD.prc`, `BremHqqQCD.prc` prepare the corresponding amplitudes for $W \to qq$, $Z \to qq$, $H \to qq$ processes . Procedures `SoftWqqQCD.prc`, `SoftZqqQCD.prc`, `SoftHqqQCD.prc` calculate the soft gluon bremsstrahlung contributions analytically. Procedures `HardWqqQCD.prc`, `HardZqqQCD.prc`, `HardHqqQCD.prc` prepare fully differential expressions of hard gluon bremsstrahlung contributions. These expressions may be used by Monte Carlo generators (or integrators). The *Hard* procedures continue the analytical calculation of hard gluon contributions by integrating over the angle between one of the quarks and the gluon and over the invariant mass of the final particles.

Here we present QCD corrections to boson decays. Analytical expressions are too cumbersome to be presented in this paper. One can access these results in the system. Here we cast the corrected decays width in the form

$$\Gamma^{\text{1loop}} = \Gamma^{\text{Born}} \left[1 + \delta(m_b, m_{q_1}, m_{q_2})\right], \tag{4}$$

where m_b, m_{q_1} and m_{q_2} are the masses of the boson and two quarks and δ is the correction.

In regard to vector boson decays everything is straightforward. In the Table 1 we give one-loop numerical results for the function $\delta(m_V, m_{q_1}, m_{q_2})$ in percent, where m_V is the mass of the vector bosons.

The well known formula for vector boson decay into massless quarks is:

$$\delta(m_V, 0, 0) = \frac{3}{4} C_f \frac{\alpha_s}{\pi}, \qquad C_f = \frac{4}{3}, \tag{5}$$

process	$\delta(m_b, m_{q1}, m_{q2})$	%
$W \to c\bar{s}$	$\delta(m_W, m_c, m_s)$	+3.44
$Z \to b\bar{b}$	$\delta(m_Z, m_b, m_b)$	+3.88
$Z \to u\bar{u}$	$\delta(m_Z, m_u, m_u)$	+3.41

Table 1: Function $\delta(m_V, m_{q1}, m_{q2})$ in percent.

which gives 3.41% for all decays of vector bosons. One can see that our numbers are in a good agreement with the classic result. However, mass effects are significant.

QCD radiative corrections to the Higgs boson decay into a quark pair have been considered earlier by one of the authors in Ref. [3]. There the one-loop QCD correction was presented keeping the masses of the outgoing quarks (Eq. 4.1) and neglecting these masses everywhere except in logarithms (Eq. 4.3). The latter equation reads

$$\delta(m_H, m_q \simeq 0, m_q \simeq 0) = C_f \frac{\alpha_s}{\pi} \left[\frac{9}{4} + \frac{3}{2} \ln\left(\frac{m_q^2}{M_H^2}\right)\right]. \tag{6}$$

In the framework of SANC we reproduced this result. The term with the large logarithm

$$C_f \frac{\alpha_s}{\pi} \left[\frac{3}{2} \ln\left(\frac{m_q^2}{M_H^2}\right)\right] \tag{7}$$

was obtained first and discussed in Ref. [4]. It doesn't violate the Kinoshita-Lee-Nauenberg theorem since the Higss-quark coupling constant is proportional to the quark mass. Moreover, resummation of these large logarithms in all orders of the perturbation theory is possible as suggested in Ref. [4].

4 QCD radiative corrections to semi-leptonic top quark decay

Here we discuss in detail the analytic calculation of QCD radiative corrections to the semi-leptonic mode of the top quark decay $t \to b\ell^+\nu_\ell$.

First we consider the easier calculation of the cascade top decay: $t \to bW^+$ followed by $W^+ \to \ell^+\nu_\ell$ using the following formula for the top decay width:

$$\Gamma_{t\to b\ell^+\nu_\ell} = \frac{\Gamma_{t\to bW^+}\, \Gamma_{W^+\to\ell^+\nu_\ell}}{\Gamma_W}, \tag{8}$$

where Γ_W is total width of the W boson. The QCD corrections are present only in the partial width $\Gamma_{t\to bW^+}$ of the top quark.

decay	$t \to bW^+$	$W^+ \to e^+\nu_e$	$t \to be^+\nu_e$ cascade
$\Gamma^{\rm Born}$	1.5930	0.22018	0.16405
$\Gamma^{\rm 1loop}$	1.4764	0.22018	0.15204
$\delta, \%$	- 7.32	0	-7.32

Table 2: Cascade approximation for QCD corrections to the top quark decay $t \to be^+\nu_e$.

4.1 QCD radiative correction to decay $t \to bW^+$

This mode of the top decay is treated in `SANC` in the same way as the **b2q** decays considered in the previous section. The virtual part of QCD corrections to the decay $t \to bW^+$ is similar to that of the decay $W^- \to d\bar{u}$. One can prepare it by the procedure `VirtTopWbQCD.prc` and then calculate the gluon bremsstrahlung contribution using procedures specific for decay $t \to bW^+$: `BremTopWbQCD.prc`, `SoftTopWbQCD.prc`, `HardTopWbQCD.prc`.

The authors of the Ref. [5] have studied the effects of the total width Γ_W in cascade calculations. But gluons are not emitted from the W boson, so the QCD correction to the decay $t \to bW^+$ does not depend on Γ_W. Results of the narrow width cascade approximation for QCD corrections to the top quark decay $t \to be^+\nu_e$ are given in Table 2.

We see that the QCD correction to $\Gamma_{t\to b\ell^+\nu_\ell}$ is the same as the QCD correction to $\Gamma_{t\to bW^+}$. This is so because according to the formula (8) we have

$$\Gamma_{t\to b\ell^+\nu_\ell} = \frac{\Gamma^{\rm Born}_{t\to bW^+}\,(1+\delta)\,\Gamma_{W^+\to\ell^+\nu_\ell}}{\Gamma_W} = \Gamma^{\rm Born}_{t\to b\ell^+\nu_\ell}\,(1+\delta). \tag{9}$$

4.2 One-loop QCD amplitude of decay $t \to b + \ell^+ + \nu_\ell$

The one-loop QCD amplitude comes from the following gauge independent set of diagrams:

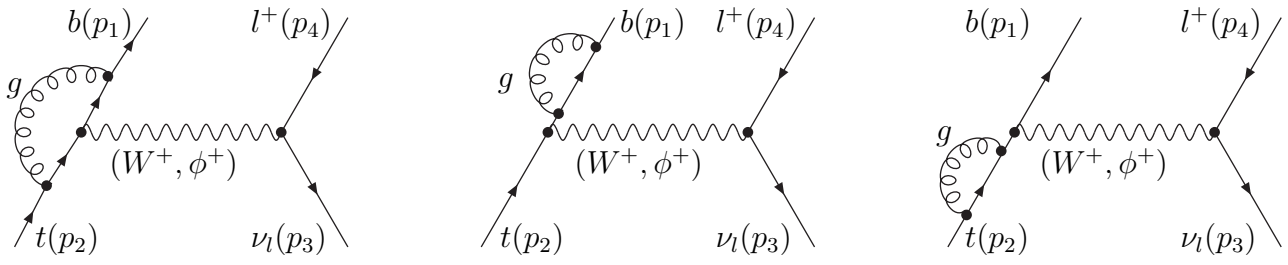

Figure 4: One-loop QCD diagrams of t quark decay: vertex and two counter terms.

The QCD part of the amplitude has the same structure as the electroweak one (see Ref. [1]):

$$\mathcal{A} = V_{tb}\,\frac{g^2}{8}\,\bar{U}_b(p_1)\,\Big[\qquad +i\,\gamma_\mu\,(1+\gamma_5)\,\mathcal{F}^{\rm QCD}_{LL}(s) + i\,\gamma_\mu\,(1-\gamma_5)\,\mathcal{F}^{\rm QCD}_{RL}(s)$$

$$+D_\mu\,(1+\gamma_5)\,\mathcal{F}_{LD}^{\rm QCD}(s)\;+D_\mu\,(1-\gamma_5)\,\mathcal{F}_{RD}^{\rm QCD}(s)\,\Big]\,U_t(p_2)$$
$$\times\frac{1}{s-\widetilde{M}_W^2}\;\bar{U}_{\nu_l}(p_3)\,\gamma_\mu\,(1+\gamma_5)\;V_l(p_4). \tag{10}$$

Here D_μ and 4-momentum conservation read

$$D_\mu=(p_1+p_2)_\mu\,,\quad p_2=p_1+p_3+p_4\,, \tag{11}$$

the invariant s (in the Pauli metric) is

$$s=-(p_2-p_1)^2, \tag{12}$$

V_{tb} is the element of the CKM matrix; $\bar{U}$, U and V are the corresponding bispinors.

Form factors obtained by FORM code **FF** (see Fig. 1) are already free from ultraviolet divergences:

$$\begin{aligned}
\mathcal{F}_{LL}^{\rm QCD}(s) &= C_f\frac{\alpha_s}{4\pi}\left[\ln\left(\frac{m_t^2}{m_g^2}\right)+\ln\left(\frac{m_b^2}{m_g^2}\right)-2\,(m_t^2+m_b^2-s)\,C_0(-m_t^2,-m_b^2,-s;m_t,m_g,m_b)\right.\\
&\left.+\left(\frac{1}{\beta(m_t^2,m_b^2,s)}-\frac{\sqrt{\lambda(s,m_t^2,m_b^2)}}{2s}\right)L\left(m_t^2,m_b^2,s\right)-4-\frac{m_t^2-m_b^2}{2s}\,\ln\left(\frac{m_b^2}{m_t^2}\right)\right],\\
\mathcal{F}_{RL}^{\rm QCD}(s) &= C_f\frac{\alpha_s}{2\pi}\,\frac{m_t m_b}{\sqrt{\lambda(s,m_t^2,m_b^2)}}\,L\left(m_t^2,m_b^2,s\right),\\
\mathcal{F}_{RD}^{\rm QCD}(s) &= -C_f\frac{\alpha_s}{8\pi}\,\frac{m_t}{s}\left[\ln\left(\frac{m_b^2}{m_t^2}\right)+\frac{1}{\beta(m_t^2,-s,m_b^2)}L\left(m_t^2,m_b^2,s\right)\right],\\
\mathcal{F}_{LD}^{\rm QCD}(s) &= C_f\frac{\alpha_s}{8\pi}\,\frac{m_b}{s}\left[\ln\left(\frac{m_b^2}{m_t^2}\right)+\frac{1}{\beta(m_t^2,s,m_b^2)}L\left(m_t^2,m_b^2,s\right)\right],
\end{aligned} \tag{13}$$

where

$$\begin{aligned}
\lambda(s,m_t^2,m_b^2)&=s^2+m_t^4+m_b^4-2sm_t^2-2sm_b^2-2m_t^2m_b^2,\\
\beta(m_t^2,m_b^2,s)&=\frac{\sqrt{\lambda(s,m_t^2,m_b^2)}}{m_t^2+m_b^2-s},\qquad \beta(m_t^2,s,m_b^2)=\frac{\sqrt{\lambda(s,m_t^2,m_b^2)}}{m_t^2+s-m_b^2},\\
\beta(m_t^2,-s,m_b^2)&=\frac{\sqrt{\lambda(s,m_t^2,m_b^2)}}{m_t^2-s-m_b^2},\qquad L\,(x,y,z)=\ln\frac{1+\beta(x,y,z)}{1-\beta(x,y,z)}.
\end{aligned} \tag{14}$$

The gluon infrared singularity is regularized by a fictitious gluon mass m_g. The Passarino-Veltman function $C_0(-m_t^2,-m_b^2,-s;m_t,m_g,m_b)$ is infrared singular. The lepton mass is neglected.

The helicity amplitudes for this mode of top quark decay are the same as those given in [1] but we have to take QCD form factors $\mathcal{F}_{LL}^{\rm QCD}(s)$, $\mathcal{F}_{RL}^{\rm QCD}(s)$, $\mathcal{F}_{LD}^{\rm QCD}(s)$ and $\mathcal{F}_{RD}^{\rm QCD}(s)$ instead of EW ones.

4.3 Virtual QCD correction

The three particle phase space element is

$$d\Phi^{(3)} = \frac{ds}{2\pi}\,\frac{\sqrt{\lambda(s,m_t^2,m_b^2)}}{8\pi m_t^2}\quad \frac{d\cos\vartheta_l}{16\pi} \;=\; \frac{ds\;du}{128\pi^3\,m_t^2}, \tag{15}$$

where the invariant u is related to the angle ϑ_l between the lepton momentum $\vec{p_4}$ in the R-frame ($\vec{p_3}+\vec{p_4}=0$) and the momentum $\vec{p_1}$ of the b quark, as follows:

$$u = \frac{1}{2}\left[m_t^2 + m_b^2 - s + \sqrt{\lambda(s,m_t^2,m_b^2)}\cos\vartheta_l\right]. \tag{16}$$

The angle ϑ_l varies from 0 to π and the invariant s varies in the interval

$$0 \;\le\; s \;\le\; (m_t - m_b)^2. \tag{17}$$

Using the formula

$$d\Gamma = \frac{1}{2m_t}\mid V_{tb}\mid^2\mid \mathcal{A}\mid^2 d\Phi^{(3)}, \tag{18}$$

we obtain the differential width of the top quark decay in the Born approximation

$$\frac{d^2\Gamma_0(s,u)}{ds\,du} = \mid V_{tb}\mid^2\frac{G_F^2}{16\pi^3 m_t^3}\;\frac{M_W^4}{\mid s-\widetilde{M}_W^2\mid^2}\;\left(m_t^2-u\right)\left(u-m_b^2\right). \tag{19}$$

Integration over the invariant u (i.e. over the angle ϑ_l) gives

$$\frac{d\Gamma_0(s)}{ds} = \mid V_{tb}\mid^2\frac{G_F^2}{96\pi^3 m_t^3}\;\frac{M_W^4\sqrt{\lambda(s,m_t^2,m_b^2)}}{\mid s-\widetilde{M}_W^2\mid^2}\;\left[\left(m_t^2-m_b^2\right)^2 + s\left(m_t^2+m_b^2\right) - 2s^2\right]. \tag{20}$$

The virtual QCD correction $\dfrac{d^2\Gamma_{\rm Virt}(s,u)}{ds\,du}$ is obtained by the procedure `VirtTop3fQCD.prc` using formula (18) but with the one–loop amplitude. It can be integrated numerically using Eq. (1). The analytic expression is too cumbersome to be given here; it can be accessed on-line in SANC.

4.4 Gluon bremsstrahlung corrections

The gluon bremsstrahlung amplitude is prepared by the procedure `BremTop3fQCD.prc`.

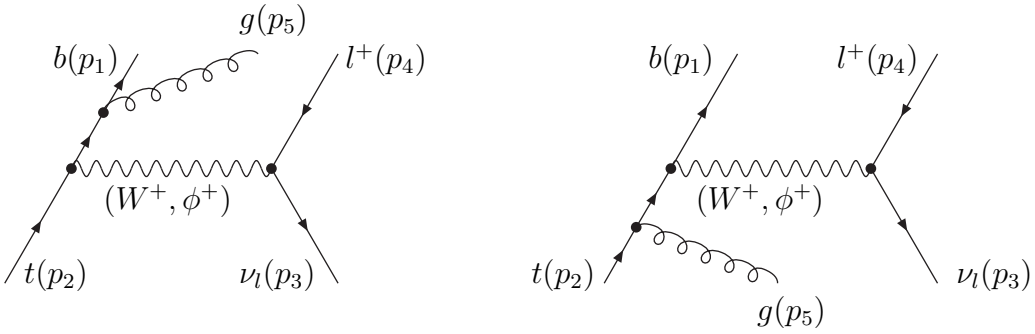

Figure 5: Gluon bremsstrahlung diagrams of t quark decay.

The conservation of 4-momentum reads

$$p_2 = p_1 + p_3 + p_4 + p_5. \tag{21}$$

An auxiliary parameter $\bar{\omega}$ separates the soft and hard gluon contributions. Gluon energy for the soft gluon bremsstrahlung lies in the limits

$$0 \le p_5^0 \le \bar{\omega}. \tag{22}$$

Therefore the soft bremsstrahlung amplitude is factorized by the Born amplitude and the kinematics of the soft bremsstrahlung is Born-like. The four-particle phase space element in this case is a product of the same three-particle phase space element $d\Phi^{(3)}$ and the phase space element of the emitted soft gluon. Integrating over the angle of the gluon emission we obtain by the procedure `SoftTop3fQCD.prc` the soft gluon contribution

$$\frac{d^2\Gamma_{\rm Soft}(s,u)}{ds\,du} = \frac{d^2\Gamma_0(s,u)}{ds\,du}\, C_f\, \frac{\alpha_s}{\pi}\, \delta_{\rm Soft}(s). \tag{23}$$

The infrared divergences here are the same as the ones in the virtual gluon contribution $\dfrac{d^2\Gamma_{\rm Virt}(s,u)}{ds\,du}$ but with the opposite sign. So, the sum of virtual and soft gluon contributions does not contain any infrared divergences. We give here the expression of this sum integrated by `IntcTop3fQCD.prc` over the invariant u

$$\begin{aligned}
\frac{d\Gamma_{\rm Virt}(s)}{ds} \;+\; \frac{d\Gamma_{\rm Soft}(s)}{ds} = \frac{d\Gamma_0(s)}{ds}\; C_f\, \frac{\alpha_s}{2\pi} \Bigg\{ & \ln\left(\frac{4\,\bar{\omega}^2}{s}\right) \left[\frac{1}{\beta\,(m_t^2, m_b^2, s)} L(m_t^2, m_b^2, s) - 2\right] \\
& + \ln\left(\frac{m_t^2}{s}\right) \left[\frac{1}{\beta(m_t^2, m_b^2, s)}\, L(m_t^2, s, m_b^2) + \frac{m_t^2}{2s} - \frac{m_b^2}{2s} + 1\right] \\
& - \ln\left(\frac{m_b^2}{s}\right) \left[\frac{1}{\beta(m_t^2, m_b^2, s)}\, L(m_t^2, -s, m_b^2) + \frac{m_t^2}{2s} - \frac{m_b^2}{2s} - 1\right]
\end{aligned}$$

$$
\begin{aligned}
&+\frac{1}{\beta(m_t^2,m_b^2,s)}\left[L^2(m_t^2,s,m_b^2)+4\,\mathrm{Li}_2\left(\frac{2\beta(m_t^2,s,m_b^2)}{1+\beta(m_t^2,s,m_b^2)}\right)\right]\\
&-\frac{1}{\beta(m_t^2,m_b^2,s)}\left[L^2(m_t^2,-s,m_b^2)+4\,\mathrm{Li}_2\left(\frac{2\beta(m_t^2,-s,m_b^2)}{1+\beta(m_t^2,-s,m_b^2)}\right)\right]\\
&+\frac{1}{\beta(m_t^2,m_b^2,s)}\,L(m_t^2,m_b^2,s)+\frac{1}{\beta(m_t^2,-s,m_b^2)}\,L(m_t^2,-s,m_b^2)\\
&+\frac{1}{\beta(m_t^2,s,m_b^2)}\,L(m_t^2,s,m_b^2)-4\\
&-\left(\frac{\sqrt{\lambda(s,m_t^2,m_b^2)}}{2s}+\frac{m_t m_b}{\sqrt{\lambda(s,m_t^2,m_b^2)}}\right)L(m_t^2,m_b^2,s)\Bigg\}\\
&-\mid V_{tb}\mid^2\frac{G_F^2\,m_b}{64\pi^3 m_t^2}\frac{C_f\alpha_s}{\pi}\frac{s\,(s-m_t^2-m_b^2+4m_t m_b)\,M_W^4}{\mid s-\widetilde{M}_W^2\mid^2}\;L(m_t^2,m_b^2,s).
\end{aligned}
\tag{24}
$$

The hard gluon contribution is produced by the procedure `HardTop3fQCD.prc`. The gluon energy p_5^0 for the hard gluon bremsstrahlung varies in the interval

$$
\bar{\omega}\;\le\;p_5^0\;\le\;max(p_5^0). \tag{25}
$$

The four particle phase space element is

$$
d\Phi^{(4)}=\frac{ds}{128\pi^3\,m_t^2}\;\frac{\sqrt{\lambda(s,m_t^2,m_b^2)}}{128\pi^3 s}\;\;(s-s')\;ds'\,d\cos\vartheta_1\,d\cos\vartheta_4 d\varphi_4, \tag{26}
$$

where s' is the invariant mass of the two final leptons, $s'=-(p_3+p_4)^2$. It varies in the interval (neglecting the mass of charged lepton):

$$
0\;\le\;s'\;\le\;s-2\bar{\omega}\,\sqrt{s}. \tag{27}
$$

The separating parameter $\bar{\omega}$ is arbitrary small. The sum of soft and hard gluon contribution to the decay width has no trace of it.

The kinematics and choice of variables to be integrated over are illustrated in Fig. 6. The angle ϑ_1 is between the b quark momentum ($\vec{p_1}$) and the emitted gluon momentum ($\vec{p_5}$), the angle ϑ_4 is between charged lepton momentum ($\vec{p_4}$) and emitted gluon momentum ($\vec{p_5}$). The z-axis is chosen here along the momentum $\vec{p_5}$ of the emitted gluon.

Using a formula analogous to (18) we obtain the fully differential hard gluon contribution to the top quark decay. After integration over angles we get

$$
\begin{aligned}
\frac{d^2\Gamma_{\mathrm{Hard}}(s,s')}{ds\,ds'} &= \frac{d\Gamma_0(s)}{ds}\,\frac{C_f\,\alpha_s}{\pi\,(s-s')}\,\frac{\mid s-\widetilde{M}_W^2\mid^2}{\mid s'-\widetilde{M}_W^2\mid^2}\left[\frac{1}{\beta(m_t^2,m_b^2,s)}\,L(m_t^2,m_b^2,s)-2\right]\\
&+ \mid V_{tb}\mid^2\frac{G_F^2}{96\pi^3 m_t^3}\,\frac{C_f\,\alpha_s}{\pi}\;\frac{M_W^4}{\mid s'-\widetilde{M}_W^2\mid^2}
\end{aligned}
$$

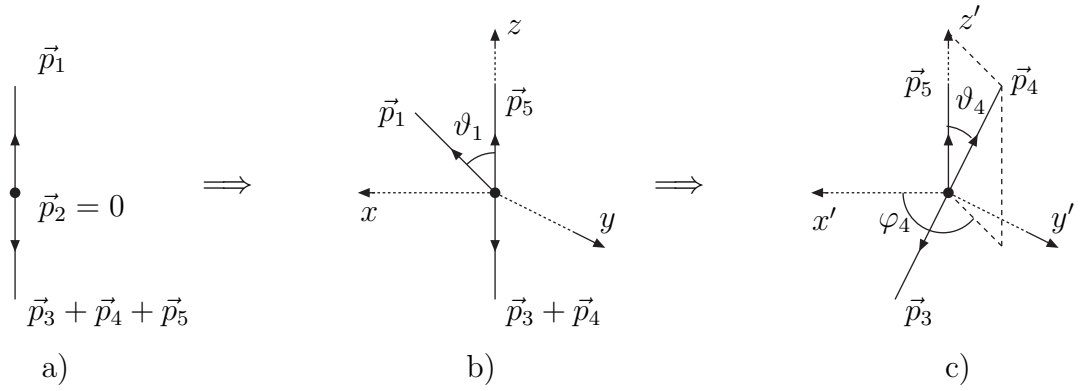

Figure 6: a) Lab. system; b) Rest system $\vec{p}_3 + \vec{p}_4 + \vec{p}_5 = 0$; c) Rest system $\vec{p}_3 + \vec{p}_4 = 0$.

$$\times\Bigg\{ \quad - \quad \left[(m_t^2+m_b^2)^2 - (m_t^2+m_b^2)\left(\frac{7}{2}s+\frac{3}{2}s'\right) + 2s^2 + ss' + s'^2\right] L(m_t^2, m_b^2, s)$$
$$+ \quad \frac{2}{s}\sqrt{\lambda(s,m_t^2,m_b^2)}\left[s(m_t^2+m_b^2) - (2s^2+ss'+s'^2)\right]\Bigg\}. \qquad (28)$$

Neglecting the mass of the charged lepton we obtain the QCD radiative correction to the decay width:

$$\begin{aligned} \Gamma_{t\to b\ell^+\nu_\ell} &= \Gamma^{\rm Born}_{t\to b\ell^+\nu_\ell}\,(1+\delta), \\ \delta &= -8.48\%. \end{aligned} \qquad (29)$$

Our result is in agreement with the result of Ref. [6] ($\delta = -8.5\%$).

Comparing the narrow width cascade approximation result in Table 2 with the complete result (29) we see that the QCD radiative correction to the decay width obtained by the narrow width formula (9) is near but not equal to the complete result.

5 QCD radiative corrections to Drell–Yan processes

Here we present the results for the corrections to the charged (CC) and neutral (NC) current Drell–Yan processes, $u\bar{d} \to \ell^+\nu_\ell$ and $q\bar{q} \to \ell^+\ell^-$, respectively. All formulas below are shown at the partonic level.

At first we give expressions for cross sections in the Born approximation:

$$\begin{aligned} \hat{\sigma}_0^{\rm CC}(s) &= |\,V_{ud}\,|^2 \frac{G_F^2}{18\pi}\,\frac{M_W^4}{|\,s-\widetilde{M}_W^2\,|^2}\,\left(s - \frac{3}{2}m_\ell^2 + \frac{m_\ell^6}{2s^2}\right), \\ \hat{\sigma}_0^{\rm NC}(s) &= \beta(s,m_\ell^2,m_\ell^2)\left[\frac{4}{9s}\left(1-\frac{m_\ell^2}{s}\right)V_0(s) + \frac{4m_\ell^2}{3s^2}V_a(s)\right], \end{aligned} \qquad (30)$$

where $s = -(p_1+p_2)^2$, p_1 and p_2 are 4-momenta of the initial quarks; $\beta(s,m_\ell^2,m_\ell^2) =$

$\sqrt{1-\dfrac{4m_\ell^2}{s}}$; m_ℓ is the lepton mass. Here we denote

$$\begin{aligned}
V_0(s) &= Q_q^2Q_\ell^2 + Q_qQ_\ell\left[\chi_Z(s)+\chi_Z^*(s)\right]v_qv_\ell + |\,\chi_Z(s)\,|^2\left(v_q^2+{I_q^{(3)}}^2\right)\left(v_\ell^2+{I_\ell^{(3)}}^2\right),\\
V_a(s) &= V_0(s) - 2|\,\chi_Z(s)\,|^2\left(v_q^2+{I_q^{(3)}}^2\right)\left(I_\ell^{(3)}\right)^2,\\
&\quad v_q = I_q^{(3)} - 2Q_q\sin^2\theta_W, \qquad v_\ell = I_\ell^{(3)} - 2Q_\ell\sin^2\theta_W. \qquad (31)
\end{aligned}$$

The Z/γ propagator ratio $\chi_Z(s)$ with s–dependent (or constant) Z width is given in [7].

The one-loop QCD amplitude of the charged current Drell–Yan process is similar to (10) given in the previous section and the corresponding amplitude of the neutral current Drell–Yan process has another form. However, we neglect the terms proportional to the masses of the initial quarks and therefore the virtual QCD corrections of both processes calculated in corresponding procedures `VirtCC4fQCD.prc` and `VirtNC4fQCD.prc` are proportional to corresponding Born cross sections.

The gluon bremsstrahlung amplitudes both for CC and NC processes are prepared by the procedure `Brem4fQCD.prc`. Here we give the sum of soft and virtual gluon contributions which does not contain any infrared divergences.

$$\begin{aligned}
\hat\sigma^{\rm CC}_{\rm Virt}+\hat\sigma^{\rm CC}_{\rm Soft} &= \hat\sigma_0^{\rm CC}(s)\;C_f\,\frac{\alpha_s}{2\pi}\Bigg\{\ln\left(\frac{4\bar\omega^2}{s}\right)\left[\ln\left(\frac{s}{m_u^2}\right)+\ln\left(\frac{s}{m_d^2}\right)-2\right]\\
&\qquad +\frac{3}{2}\ln\left(\frac{s}{m_u^2}\right)+\frac{3}{2}\ln\left(\frac{s}{m_d^2}\right)-4-\frac{\pi^2}{3}\Bigg\}, \qquad (32)\\
\hat\sigma^{\rm NC}_{\rm Virt}+\hat\sigma^{\rm NC}_{\rm Soft} &= \hat\sigma_0^{\rm NC}(s)\;C_f\,\frac{\alpha_s}{\pi}\Bigg\{\ln\left(\frac{4\bar\omega^2}{s}\right)\left[\ln\left(\frac{s}{m_q^2}\right)-1\right]\\
&\qquad +\frac{3}{2}\ln\left(\frac{s}{m_q^2}\right)-2-\frac{\pi^2}{6}\Bigg\}, \qquad (33)
\end{aligned}$$

where m_q, m_u, m_d are quark masses. Hard and soft gluon bremsstrahlung contributions are calculated in procedures `SoftCC4fQCD.prc`, `HardCC4fQCD.prc` for CC and `SoftNC4fQCD.prc`, `HardNC4fQCD.prc` for NC, respectively. We present here expressions for hard bremsstrahlung with extracted splitting function:

$$\begin{aligned}
\frac{d\hat\sigma^{\rm CC}_{\rm Hard}}{ds'} &= \hat\sigma_0^{\rm CC}(s')\;C_f\,\frac{\alpha_s}{2\pi}\frac{1}{s^2}\frac{s^2+s'^2}{s-s'}\left[\ln\left(\frac{s}{m_u^2}\right)+\ln\left(\frac{s}{m_d^2}\right)-2\right], \qquad (34)\\
\frac{d\hat\sigma^{\rm NC}_{\rm Hard}}{ds'} &= \hat\sigma_0^{\rm NC}(s')\;C_f\,\frac{\alpha_s}{\pi}\frac{1}{s^2}\frac{s^2+s'^2}{s-s'}\left[\ln\left(\frac{s}{m_q^2}\right)-1\right], \qquad (35)
\end{aligned}$$

where s' is the invariant mass of final leptons.

One-loop radiative corrections contain terms proportional to logarithms of the quark masses, $\ln\left(\dfrac{s}{m_q^2}\right)$. They come from the initial state radiation contribution including virtual, soft and hard gluon emission. In the case of hadron collisions these logarithms have

been already taken into account in the parton density functions (PDF's). Therefore we have to apply a subtraction scheme to avoid the double counting. Linearization of the subtraction procedure is done as described in the Ref. [8].

In order to have the possibility to impose experimental cuts and event selection procedures of any kind, we use a Monte Carlo integration routine based on the Vegas algorithm [9]. In this case we perform a 4(6)-fold numerical integration to get the hard gluon contribution to the partonic (hadronic) cross sections. To get the one-loop QCD corrections we add also the contributions of the soft gluon emission and the one of the virtual QCD loops. The cancellation of the dependence on the auxiliary parameter $\bar{\omega}$ in the sum is observed numerically.

For numerical evaluations we take the same set of input parameters as the one given in Ref. [10].

At Fig. 7 we present the neutrino–lepton pair transverse mass distribution of cross section for Drell–Yan CC process. The hard and soft-virtual contributions are huge, but they cancel each other, see Fig. 7a). The total QCD correction shown at Fig. 7b) is very small. Comparison of QCD and EW distributions was discussed in reports on workshop [11].

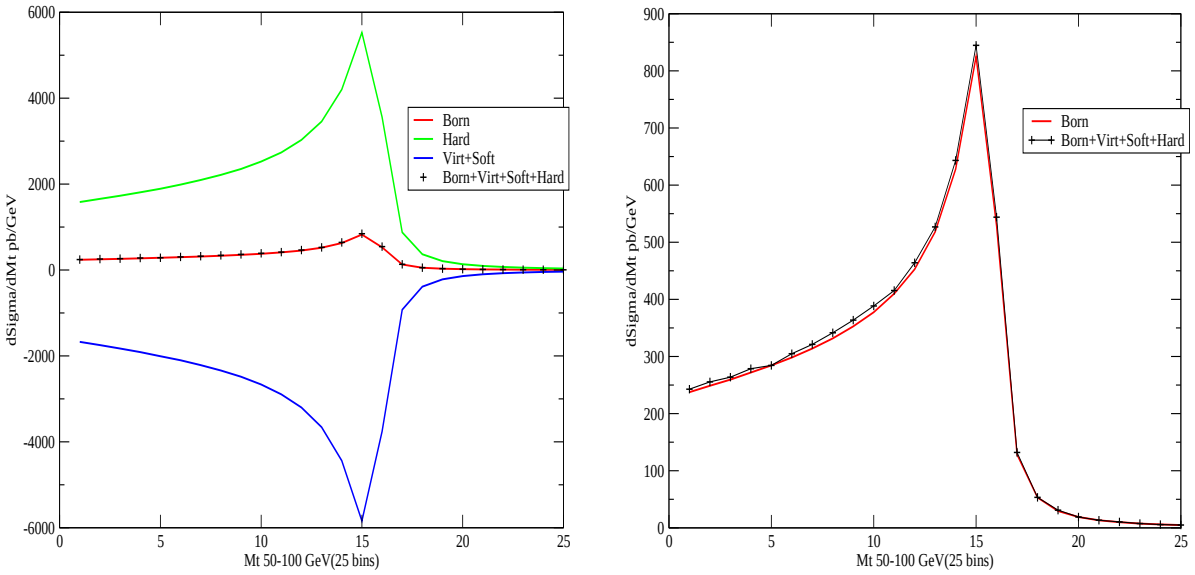

Figure 7: Transverse mass M_t of neutrino–lepton pair distribution for Drell–Yan CC.

At Fig. 8a) we show the lepton pair transverse momentum distribution for Drell–Yan NC process. The total QCD correction to the cross-section is small, however the shape of distribution changes greatly. At Fig. 8b) we present invariant mass of lepton pair distribution for this process.

We are going to develop a Monte Carlo event generator to describe the Drell–Yan processes in realistic conditions.

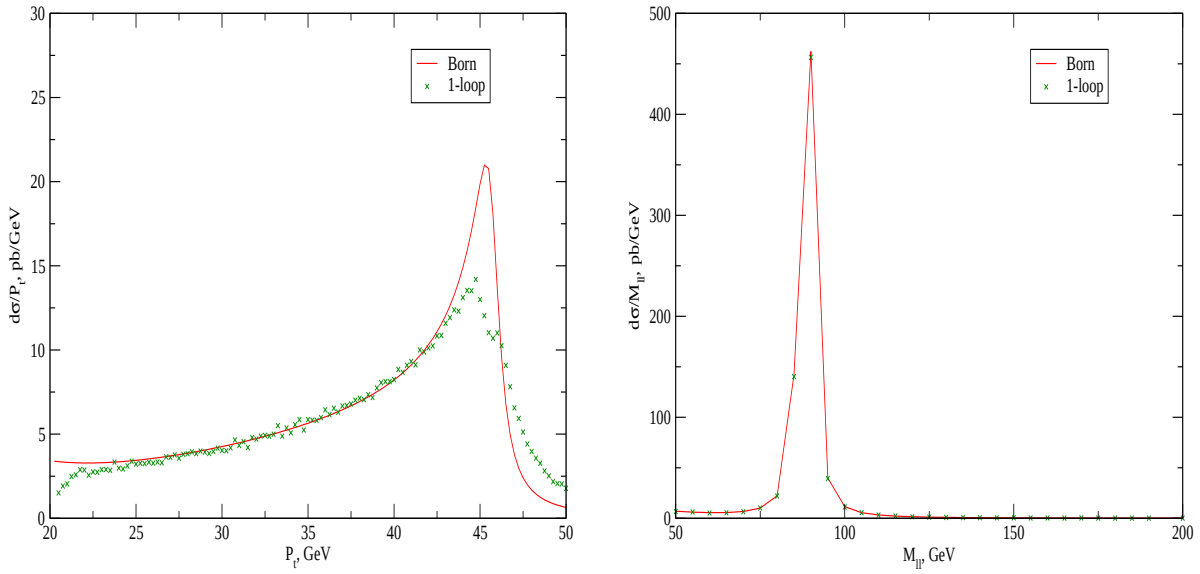

a) *b)*

Figure 8: Transverse momentum P_t and invariant mass M_{ll} of lepton pair distributions for Drell–Yan NC.

6 Summary

In this paper we described the first steps of creation of the QCD branch in the SANC system. We developed environment for calculations of QCD processes. Then we tested successfully this environment by simple calculations of **b2q** decays. We implemented corrections to top quark decays and observed that complete one–loop result differs from the narrow width cascade approximation result. Drell–Yan NC and CC processes were implemented into SANC, and we created the Monte Carlo integrators to study them. We are going to develop unified event generator for Drell–Yan processes, which would include QCD and EW corrections simultaneously.

Acknowledgments

We are grateful to D. Bardin, L. Kalinovskaya, W. von Schlippe for critical reading and discussions of this paper. This work was partially supported by the INTAS grant 03-41-1007 and by the RFBR grant 04-02-17192.

References

[1] A. Andonov et al. Comput.Phys.Commun. **174** (2006) 481 hep-ph/0411186.

[2] J.A.M. Vermaseren.*New features of* FORM. math-ph/0010025.

[3] D. Bardin, B. Vilensky, P. Christova. Sov.J.Nucl.Phys. **53** (1991) 152.

[4] E. Braaten, J.P. Levelle. Phys.Rev. **D22** (1980) 715.

[5] A. Arbuzov, D. Bardin, S. Bondarenko, P. Christova, L. Kalinovskaya and R. Sadykov. *SANCnews: Sector* $4f$*, Charged Current*. In preparation.

[6] M. Fischer, S. Groote, J.G. Koerner and M.C. Mauser. Phys.Rev. **D65** (2002) 054036 hep-ph/0101322.

[7] A. Andonov et al. Phys.Part.Nucl. **34** (2003), 577. Fiz.Elem.Chast.Atom.Yadra **34**, (2003) 1125, hep-ph/0207156.

[8] A. Arbuzov et al. Eur.Phys.J. **C 46** (2006) 407 hep-ph/0506110.

[9] G.P. Lepage, J.Comput.Phys. **27** (1978) 192.

[10] C. Buttar et al. *Les Houches physics at TeV colliders 2005, Standard Model, QCD, EW, and Higgs working group: Summary report,* hep-ph/0604120.

[11] V. Kolesnikov, *SANC: QCD sector.* International school–workshop "Calculations for modern and future colliders", Dubna, Russia, July 15-25, 2006.